

Submitted: May 30, 2023

Revised: November 14, 2023

Accepted: March 14, 2024

Effect on annealing on the micro-structural behavior of spray deposited Al-6Si-10Pb alloys

R. Mittal ,  I. Choudhary,  R. Sehrawat,  R. Dhawan,  P.S. Singh, 

Maharishi Markandeshwar University, Mullana, India

✉ rashmimittal3@gmail.com

ABSTRACT

In the present work, the microstructural features of spray deposited Al-6Si-10Pb alloys before and after annealing at different locations of the preform have been compared with each other. XRD confirms the presence of all elements present in the Al-6Si-10Pb alloy. The optical micrographs were taken at three different regions of the preform before and after annealing predicts that the grain size is lower at the peripheral region as compared to central region. Equiaxed grain structure was observed in SEM images, with a uniform distribution of Pb and Si phase in an Al-matrix. Further, grain refinement and reduction of porosity was observed after annealing.

KEYWORDS

Al-alloys • microstructure • spray deposition • annealing

Citation: Mittal R, Choudhary I, Sehrawat R, Dhawan R, Singh PS. Subcritical growth of repolarization nuclei in polycrystalline ferroelectric films. *Materials Physics and Mechanics*. 2024;52(2): 30–37.

http://dx.doi.org/10.18149/MPM.5222024_3

Introduction

Manufacturing industry such as construction, aerospace, and automobile demand metals/alloys which possess high strength, high corrosion resistance, high stiffness, light-weight, and low thermal expansion coefficients [1–4]. Contrary, these materials should have excellent wear and abrasive resistance for their use in bearings and gear boxes [5,6]. These properties of the materials have direct impact on the performance and efficiency of the constructed machines parts. However, attaining high strength along with good ductility is still a great challenge in the metallurgy. In steel industry, achieving this objective require a complex and time-consuming process of nitriding and carburizing. Aluminum (Al) due to its superior properties and ease of casting can be suitable alternative for iron (Fe). However, casting Al alone offers new challenges of high shrinkage, low fluidity and hot tearing. Recent studies predict that alloying aluminum (Al) with various metals such as silicon (Si), manganese (Mn), magnesium (Mg), copper (Cu) and magnesium-silicide (Mg_2Si) can resolve these casting problems. For example, Al-Si alloys offer good fluidity of molten metal at lower casting temperatures in comparison to the pure metal [7–9]. However, during conventional casting the ductility of the aluminum is compromised simultaneously as the coarse silicon particles gets embedded in the Al metal. To compensate for ductility soft elements such as lead (Pb), indium (In), and tin (Sn) can be added the mixture [10]. However, due to large density differences these elements are not miscible with Al and can't be casted using simple conventional casting techniques. Alternatively, advanced casting techniques such as spray forming [11,12] can lead to the homogeneous dispersion of soft elements in Al matrix. This technique utilizes

high velocity gas jets to disintegrate the molten metal into droplets of submicron size. These small droplets contain partially solidified particles in molten metal, which acts as nucleating sites. Consequently, rapid solidification takes place which leads to homogeneous microstructures with negligible agglomeration. In case of Al-Si alloys, earlier reports suggests that size and shape of Si particles plays major role in obtaining a fine grain structure, which can be controlled by adjusting the cooling rate during solidification. Usually, faster cooling rates lead to fine microstructure. Thus, use of spray forming technique for the production of good quality Al-Si alloy is a good choice. However, due to the non-uniform gaussian distribution of the mass in the spray droplets, the obtained preform contains high level of porosity. Thus, requires further heat treatments to reduce the porosity [13,14].

The objectives of our work are (1) to obtain fully miscible Al-6Si-10Pb alloy with no segregation using spray forming technique, and (2) to study the effect of annealing on the microstructure of Al-6Si-10Pb alloy taken at different locations of the preform.

Materials and Methods

Figure 1 represents the experimental setup and the process mechanism of the spray forming technique used for the deposition of Al-6Si-10Pb alloy on a substrate. The material processing involves heating a mixture of 900 g commercially available Al-6Si alloy (see Table 1 for the detail composition) and 100 g Pb at 1123K in the crucible kept over the nozzle of the atomizer unit.

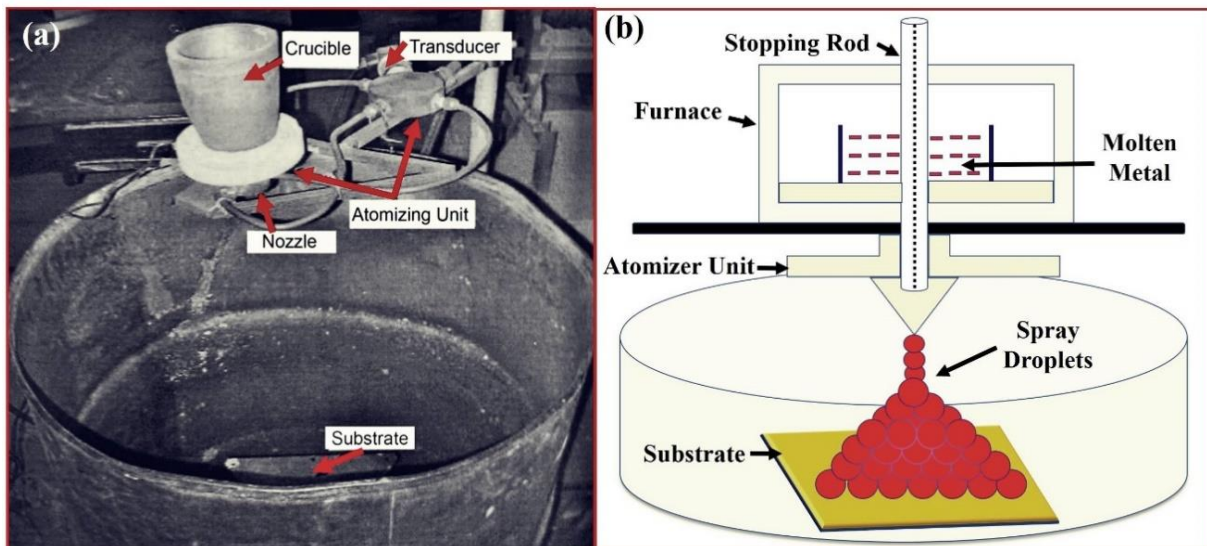


Fig. 1. (a) Photograph of the apparatus used for experimental work and (b) the process mechanism of the spray forming

Table 1. Chemical composition of Al-Si alloy

Si	Fe	Mn	Zn	Ti	Pb	Sn	Mg	Ni	Al
6.0	0.41	0.21	0.29	0.06	0.04	0.12	0.13	0.12	balance

A stopper rod at the entrance of delivery tube prevents the melt flow through it prior to its atomization. Nitrogen was supplied for atomization prior to melt flowing through the delivery tube. Atomization of melt resulted in a spray of wide range of micron size droplets. These droplets were then allowed to deposit over a copper substrate. The obtained preform was taken out of the substrate after deposition. The deposition was carried out for the alloy of composition Al-6Si-10Pb at 1123 K temperature and 1 MPa pressure of nitrogen gas. The details of the various process parameters have been listed in the Table 2.

Table 2. Process parameters used during the casting

Process parameter	Value
Melt temperature, K	1123
Atomizing gas	Nitrogen
Gas pressure, MPa	1.0
Nozzle to substrate distance, cm	35.0
Nozzle type	Convergent-divergent
Throat diameter, mm	16 (inner), 18 (outer)
Throat width, mm	1.0
Throat angle, °	5.0
Melt delivery tube diameter, mm	5.0
Substrate	Copper
Substrate diameter, mm	200.0

The spray deposited-Al-6Si-10Pb alloy was further processed through cold rolling and annealing process. The rolling operation was performed using rolling mill consisting of rollers having diameter of 110 mm and speed of 8 rpm. Several numbers of passes were applied on spray deposited Al-6Si-10Pb alloys through the rolls to achieve 40 % thickness reduction. Afterward, these samples were processed through annealing at temperature 250 °C for 1 hour. The obtained spray formed preform was characterized using X-ray diffraction (XRD), optical microscopy (OM) and scanning electron microscopy (SEM) to understand the structural and morphological properties of the Al-6Si-10Pb alloy before and after annealing. The XRD measurements Al-6Si-10Pb alloy was performed using Bruker AXS D8 Advance X-Ray Diffractometer, having Cu as target and Ni filter material. The diffraction angle (2θ) was varied from 20 to 100° with a step-size of 0.05°. The goniometer speed was kept at 2°/minute. For the observation of the microstructures, samples from the different parts of the spray formed deposits were cut down and first polished using emery paper of 1/0, 2/0, 3/0 and 4/0 specifications. Later, the samples were polished on wheel cloth polishing machine using an emulsion of alumina (Al_2O_3) particles suspended in water. Afterward, these samples were polished by kerosene oil. Lastly, these samples were etched with Keller's reagent (composition: 1 % vol. HF, 1.5 % vol. HCl, 2.5 % vol. HNO_3 and remaining water). The microstructures of samples were examined under optical microscope (Leica) and SEM (Leo-435-VP).

Results and Discussion

Structural analysis

First, the structural properties of the casted Al-6Si-10Pb alloy using XRD has been investigated. Sharp and high intensity XRD peaks (see Fig. 2) observed at diffraction angles of 38.47, 44.74, 65.13, 78.23, 82.48, and 99.08° belong to cubic lattice structure of aluminum (JCPDS card no. 04-0787) and corresponds to (111), (200), (220), (311), (222), and (400) lattice planes, respectively.

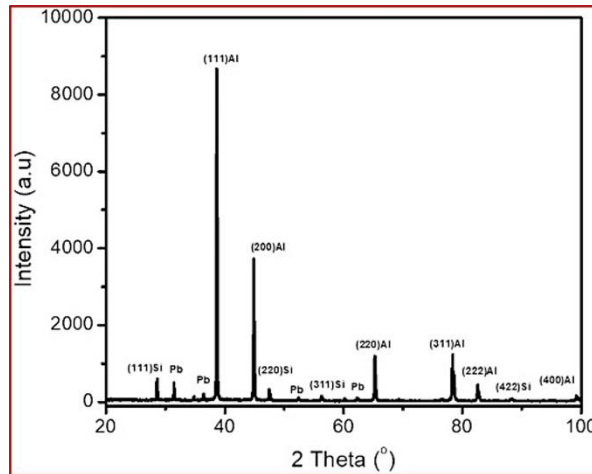


Fig. 2. XRD pattern of spray deposited Al-6Si-10Pb alloy

XRD peaks with small intensity observed at 31.31, 36.27, 52.23, and 62.12° belong to the cubic lattice structure of lead (JCPDS card no. 04-0686) and corresponds to the (111), (200), (220), and (311) lattice planes respectively. The rest of the small intensity peaks at diffraction angles of 28.44, 47.30, 56.12, and 88.03° belong to cubic silicon (JCPDS card no. 27-1402) and corresponds to the (111), (220), (311) and (422) lattice planes, respectively. This confirms the formation of Al-6Si-10Pb alloy.

Morphological analysis

Optical microscopy

Figure 3 shows the typical microstructures of the spray deposited Al-6Si-10Pb alloy, observed by optical microscopy. It is possible to recognize an equiaxial Al matrix and near-uniform distributed silicon and lead particles surrounding the Al matrix (Fig. 3(a,c,e)). The average grain size of Al is 40 μm for center and middle region (Fig. 3(a,c)) while it is lower (around 30 μm) for peripheral region (Fig. 3(e)). One of the reasons for lower grain size at peripheral region is high rate of heat transfer due to small thickness at this region reported by other researchers also [15]. Some noticeable pores are also observed in these micrographs (Fig. 3(a,c,e)). The pore size is 5-10 μm . Porosity occurs due to the high velocity gas entrapment during solidification process. However, after rolling and annealing, the porosity gets almost eliminated as can be depicted from the microstructures (Fig. 3(b,d,f)).

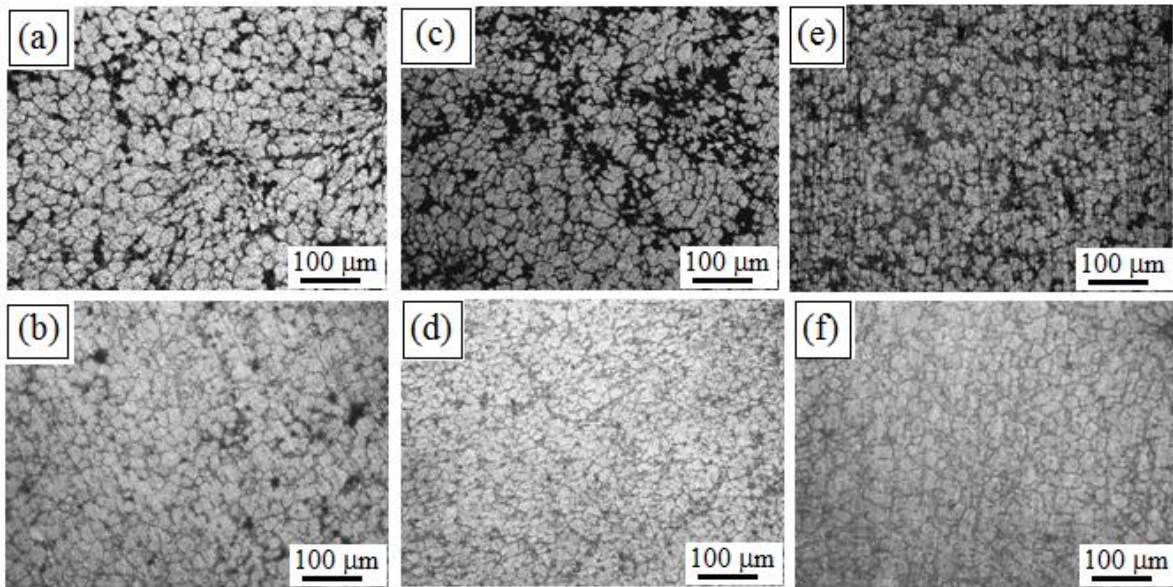


Fig. 3. Microstructure of spray deposited Al-6Si-10Pbat center region (a,b), middle region (c,d) and peripheral region (e,f) before annealing (a,c,e) and after annealing (b,d,f)

Scanning electron microscopy

Figure 4 shows SEM microstructure of the as sprayed deposit. Mostly pores are noticed at the grain boundaries. The grain boundaries due to presence of porosity have quite strained structure. The white phase shown in SEM micrograph is of silicon and grey grains are of Al matrix. The observed grain structure was homogeneous through the deposit, indicating that a good compromise between heat extraction and deposition rate was attained during deposit build-up. In addition, no banded microstructure was observed in these deposits as described by Cantor [16]. Equiaxial morphology of the Al phase was a remarkable feature of this structure and is ascribed to the extensive fragmentation and coarsening of solid phases during the build-up of the deposit. It has been assumed that during this stage of the process the solid, semisolid and fully liquid droplets impacting the surface of the deposit provide a great quantity of nuclei that coarsen due to the vigorous agitation and the cooling conditions at this solidifying layer, resulting in an equiaxial form. Concerning silicon and the intermetallic phases there are still greater differences to the conventionally cast material. In contrast to a typical eutectic as well as in spray formed hypoeutectic Al-Si alloys of others works [17,18], the silicon was identified without the appearance of a eutectic structure in this work, but as isolated particles similar to primary silicon in hypereutectic alloys. The presence of these particulate silicon has been documented by other investigators working on spray forming of eutectic and hypereutectic aluminum-silicon alloys [19,20]. The formation of the microstructure in the spray forming is frequently correlated to the situation occurring in rheo-casting because both processes show strong agitation in semi-solid state [21]. However, the rheo-cast hypoeutectic Al-Si alloys always show eutectic silicon, while the spray formed material of this work did not. The reason for this could be the significant differences between the two processes, respectively, to the cooling rate and the situation of the materials before “agitation” in semisolid state. The rheo-casting has no step which suffers rapid solidification as the atomized droplets do, it says, the solidified droplets

impact the deposit with a very fine structure and play a very important role in the subsequent microstructural development. In addition, the reheating of the deposit due to the release of latent heat is another factor in existent in rheo-casting. Indeed, the solidification conditions by spray forming of long-range freezing alloys such as A380 are difficult to be explained by classical theories of solidification, even of rapid solidification.

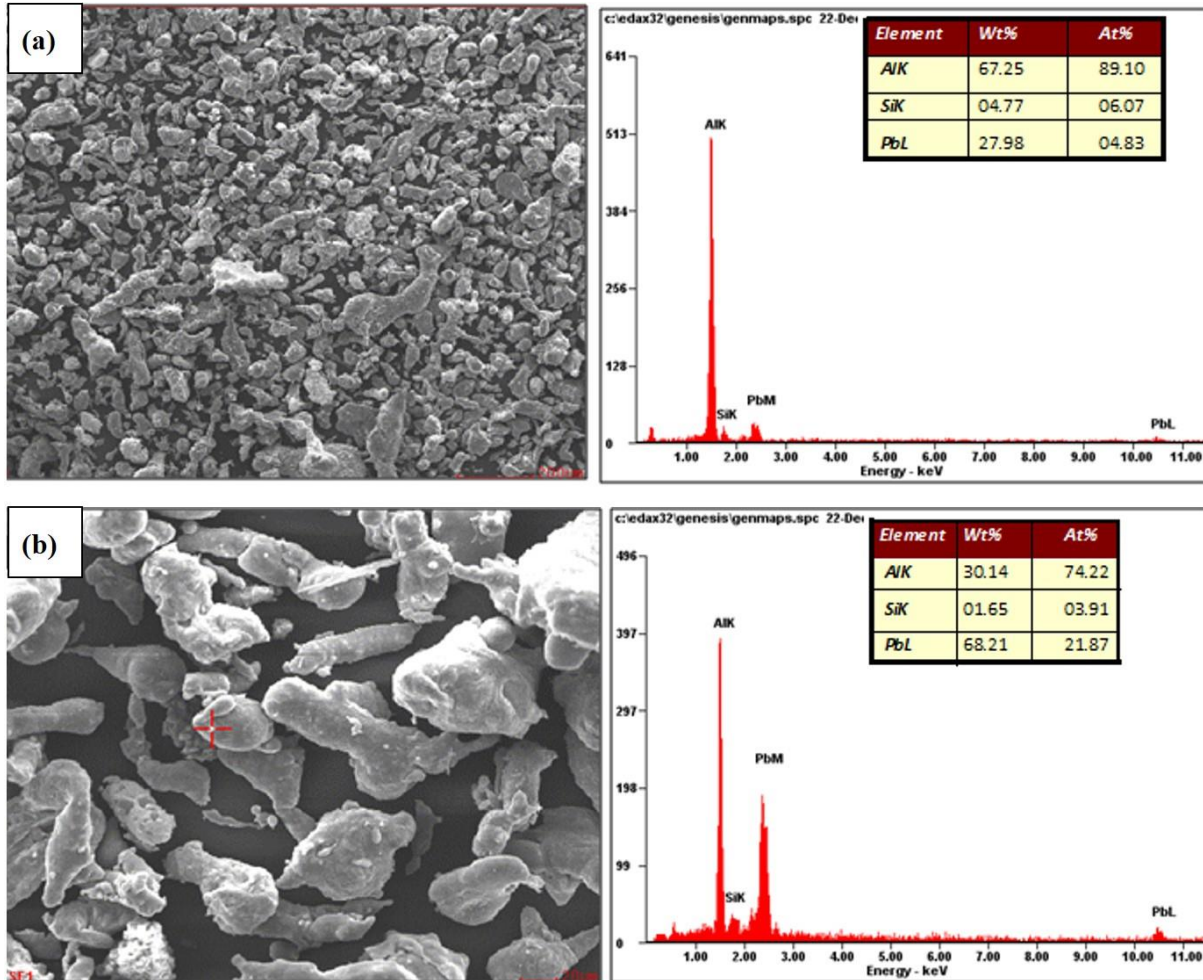


Fig. 4. SEM with EDS spectrum (a) analyzed whole region; (b) analyzed bright region, indicating Pb and Si phases in spray deposited Al-6Si-10Pb alloy

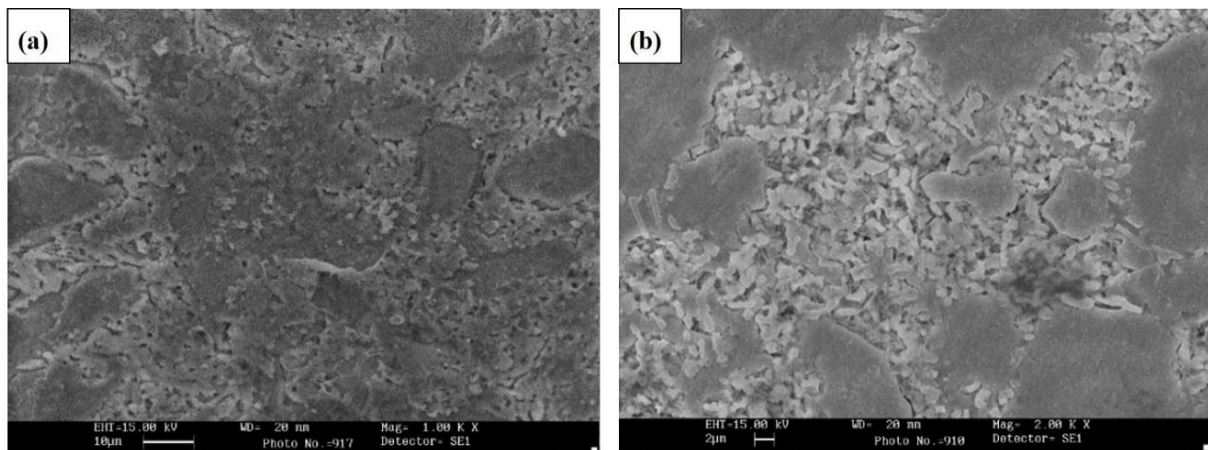


Fig. 5. SEM micrographs showing porosity at (a) 2000x; (b) 1000x

SEM micrographs showing porosity are shown in Fig. 5. The porosity formation can take place due to gas entrapment, insufficient melt to fill the porosity and solidification shrinkage. The decrease in porosity from center to periphery could be explained on the basis of decrease in gas velocity from center to periphery of the deposit. Higher gas velocity would lead to higher particle velocity at center as compared to periphery. Semi-solid particle impacting the substrate or preform at higher speed would undergo greater deformation and thus lead to lesser pores as compared to periphery where the particles would undergo less deformation leading to existence of more pores.

Conclusions

1. Al-6Si-10Pb alloy with fine equiaxed grain structure of aluminum was casted using spray forming technique.
2. Uniformly spread needle shaped silicon particles surrounding the aluminum grains were observed in the microstructure of Al-6Si-10Pb alloy.
3. The preforms at different location shows different grain size with larger grains at the center and smaller grains along the periphery. Further, high porosity was observed for the as casted preforms due to gas entrapment, and insufficient melt.
3. Rolling treatment reduces the porosity, but simultaneously generate cracks due to the applied stress. The developed stress can be reduced by using an additional annealing treatment to the Al-6Si-10Pb alloy.

References

1. Mauduit D, Dusserre G, Cutard T. Influence of temperature cycles on strength and microstructure of spray-deposited Si–Al CE9F alloy. *Mechanics of Materials*. 2019;131: 93–101.
2. Wang Y, Zhao G, Xu X, Chen X, Zhang C. Constitutive modeling, processing map establishment and microstructure analysis of spray deposited Al–Cu–Li alloy 2195. *Journal of Alloys and Compounds*. 2019;779: 735–751.
3. Goudar DM, Srivastava VC, Rudrakshi GB, Raju K, Ojha SN. Effect of Tin on the Wear Properties of Spray Formed Al–17Si Alloy. *Transactions of the Indian Institute of Metals*. 2015;68: 3–7.
4. Ramana Reddy BV, Mittal R, Maity SR, Pandey KM. Investigation on metallurgical, tribological, hardness properties of spray deposited and warm rolled Al-18Pb, Al-22Pb alloys. *Journal of Materials Research and Technology*. 2019;8: 5687–5697.
5. Milhorato FR, Mazzer EM. Effects of aging on a spray-formed Cu–Al–Ni–Mn–Nb high temperature shape memory alloy. *Materials Science and Engineering: A*. 2019;753: 232–237.
6. Ran G, Zhou J-E, Xi S, Li P. Microstructure and morphology of Al–Pb bearing alloy synthesized by mechanical alloying and hot extrusion. *Journal of Alloys and Compounds*. 2006;419: 66–70.
7. Srivastava VC, Surreddi KB, Scudino S, Schowalter M, Uhlenwinkel V, Schulz A, Rosenauer A, Zoch HW, Eckert J. Spray forming of bulk Al85Y8Ni5Co2 with co-existing amorphous, nano- and micro-crystalline structures. *Transactions of the Indian Institute of Metals*. 2009;62: 331–335.
8. Raju K, Harsha AP, Ojha SN. Microstructural Features, Wear, and Corrosion Behaviour of Spray Cast Al–Si Alloys. *Proceedings of the Institution of Mechanical Engineers, Part J: Journal of Engineering Tribology*. 2011;225: 151–160.
9. Sheinerman AG. Strengthening of nanocrystalline alloys by grain boundary segregations. *Materials Physics and Mechanics*. 2022;50(2): 193–199.
10. Mittal R, Singh D. Tribology Characteristics of Cold Rolled Spray Cast Al–6Si–20Pb Alloy. In: Patel HC, Deheri G, Patel HS. (eds.) *Proceedings of International Conference on Advances in Tribology and Engineering Systems 2014*. New Delhi, India: Springer; 2014. p.431–439.

11. Wang X, Pan Q, Liu L, Xiong S, Wang W, Lai J, Sun Y, Huang Z. Characterization of hot extrusion and heat treatment on mechanical properties in a spray formed ultra-high strength Al-Zn-Mg-Cu alloy. *Materials Characterization*. 2018;144: 131–140.
12. Mittal R, Moon AP. Effect of Rolling on the Electrochemical Corrosion Behavior of Spray Deposited Al-6Si Alloys with Different Pb Content. *Journal of Materials Engineering and Performance*. 2023;2: 7969–7979.
13. Tomar A, Mittal R, Singh D. Strength and elongation of spray formed Al-Si-Pb alloys. *International Journal of Minerals, Metallurgy, and Materials*. 2014;21: 1222–1227.
14. Singh D, Dangwal S. Effects of process parameters on surface morphology of metal powders produced by free fall gas atomization. *Journal of Materials Science*. 2006;41: 3853–3860.
15. Mittal R, Reddy BVR. Studying the Influence of Rolling Deformation Degree and Pb Content on the Hardness of Spray Deposited Al–6Si Alloy Using Linear Regression Analysis. *Powder Metallurgy and Metal Ceramics*. 2021;60: 164–173.
16. Underhill RP, Grant PS, Cantor B. Microstructure of spray-formed Al alloy 2618. *Materials & Design*. 1993;14: 45–47.
17. Gupta M, Ling S. Microstructure and mechanical properties of hypo/hyper-eutectic Al–Si alloys synthesized using a near-net shape forming technique. *Journal of Alloys and Compounds*. 1999;287: 284–294.
18. Srivastava AK, Anandani RC, Dhar A, Gupta AK. Effect of thermal conditions on microstructural features during spray forming. *Materials Science and Engineering: A*. 2001;304-306: 587–591.
19. Anand S, Srivatsan TS, Wu Y, Lavernia EJ. Processing, microstructure and fracture behaviour of a spray atomized and deposited aluminium–silicon alloy. *Journal of Materials Science*. 1997;32: 2835–2848.
20. Evstifeev AD, Chevrychkina AA, Petrov YV. Dynamic strength properties of an ultra-fine-grained aluminum alloy under tension conditions. *Materials Physics and Mechanics*. 2017;32(3): 258–261.
21. Fuxiao Y, Jianzhong C, Ranganathan S, Dwarakadasa ES. Fundamental differences between spray forming and other semisolid processes. *Materials Science and Engineering: A*. 2001;304-306: 621–626.

About Author

Rashmi Mittal  

PhD, Associate Professor (Maharishi Markandeshwar University, Mullana, India)

Ishan Choudhary  

PhD, Assistant Professor (Maharishi Markandeshwar University, Mullana, India)

Rajeev Sehrawat  

PhD, Assistant Professor (Maharishi Markandeshwar University, Mullana, India)

Rajat Dhawan  

PhD, Assistant Professor (Maharishi Markandeshwar University, Mullana, India)

Prabh Simranjit Singh  

Research Scholar (Maharishi Markandeshwar University, Mullana, India)